Electronic Supplementary Information (ESI)

Isatin N^2-diphenylhydrazones: new easily synthesized Vis-Vis molecular photoswitches

Marek Cigáň [a,*], Martin Gáplovský [b], Klaudia Jakusová [a], Jana Donovalová [a], Miroslav Horváth [a], Juraj Filo [a] and Anton Gáplovský [a]

[a] *Faculty of Natural Sciences, Institute of Chemistry, Comenius University, Mlynská dolina CH-2, SK-842 15 Bratislava, Slovakia; E-Mails: cigan@fns.uniba.sk (M.C.); jakusova@fns.uniba.sk (K.J.); donovalova@fns.uniba.sk (J.D.); horvathm@fns.uniba.sk (M.H.); sokolik@fns.uniba.sk (R.S.); gaplovsky@fns.uniba.sk (A.G.)*

[b] *Department of Pharmaceutical Chemistry, Faculty of Pharmacy, Comenius University, Odbojárov 10, SK-832 32 Bratislava, Slovakia; E-Mail: gaplovsky@fpharm.uniba.sk (M.G.)*

* cigan@fns.uniba.sk

EXPERIMENTAL SECTION – Supporting information

Synthesis

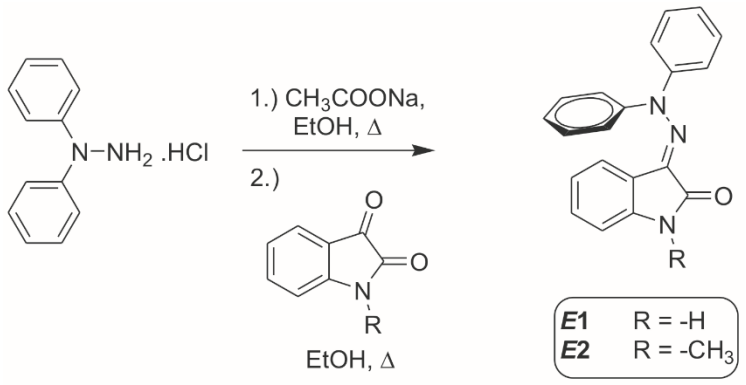

General Scheme: Synthesis of **1** and **2** *E*-isomers in EtOH.

(*E*)-isatin N^2-diphenylhydrazones 1 and 2:

(*E*)-3-(2,2-diphenylhydrazono)indolin-2-one ***E*1**:
Obtained from diphenylhydrazine (1.50g) in 82% yield (1.53g),
^{1}H NMR (300 MHz, DMSO-d_6), δ: 10.67 (s, 1H), 7.52 – 7.40 (m, 5H), 7.34 – 7.25 (m, 5H), 7.09 (ddd, J = 7.7, 1.1 Hz, 1H), 6.77 (d, J = 7.4 Hz, 1H), 6.41 (ddd, J = 7.8, 1.1 Hz, 1H), 5.41 (d, J = 7.4 Hz, 1H).
^{13}C NMR (75 MHz, DMSO-d_6) δ: 165.79 (s), 145.60 (s), 143.23 (s), 133.62 (s), 130.38 (s), 129.50 (s), 125.99 (s), 125.12 (s), 122.97 (s), 120.65 (s), 115.76 (s), 110.00 (s).
Anal. Calcd. for $C_{20}H_{15}N_3O$ (313.35) C, 76.66; H, 4.82; N, 13.41. Found C, 76.25; H, 4.78; N, 13.33.

(*E*)-3-(2,2-diphenylhydrazono)-1-methylindolin-2-one ***E*2**:
Obtained from diphenylhydrazine (1.41g) in 77% yield (1.56),
^{1}H NMR (300 MHz, $(CD_3)_2CO$), δ: 7.52 – 7.41 (m, 4H), 7.39 – 7.27 (m, 6H), 7.18 (td, J = 7.7, 1.2 Hz, 1H), 6.90 (d, J = 7.5 Hz, 1H), 6.49 (td, J = 7.7, 1.1 Hz, 1H), 5.59 (ddd, J = 7.9, 1.1, 0.5 Hz, 1H), 3.23 (s, 3H).
^{13}C NMR (75 MHz, DMSO-d_6) δ: 164.52 (s), 145.58 (s), 144.18 (s), 132.83 (s), 130.33 (s), 129.54 (s), 126.13 (s), 124.81 (s), 123.03 (s), 121.16 (s), 115.15 (s), 108.60 (s), 26.17 – 25.70 (m).
Anal. Calcd. for $C_{21}H_{17}N_3O$ (327.38) C, 77.04; H, 5.23; N, 12.84. Found C, 76.80; H, 5.11; N, 12.79.

Titration experiments

Association constant determinations
Equation (1) was rewritten to the following form for nonlinear fit:

$$A = A_0 + c_1 * (\mathrm{P1} - A_0) * (c_0 + \mathrm{x} + 1/\mathrm{P2} - \sqrt{(c_0 + \mathrm{x} + 1/\mathrm{P2})\text{^}2 - 4 * c_0 * \mathrm{x}}), \quad (2)$$

where: $c_0 = 1\times10^{-4}$, $c_1 = 1/2c_0 = 5\times10^3$, parameter P1 = A_{lim}, parameter P2 = K_{ass} and x = c_{A}-. The A_0 value was fixed to the absorbance value A for x = 0. The large difference in constants c_0, c_1 and the x-data range led rescaling the nonlinear function (x and fitted parameter 1/P2 by a factor of 10^4). Following this modification, the standard non-linear least-squares Nelder-Mead minimization method was employed to determine fitting parameters P1 and P2.[57] Three different wavelengths were used to K_{ass} determination (400 nm, 405 nm and 410 nm for isomer ***E*1**; and 420 nm, 425 nm and 430 nm for ***E*1**/ ***Z*1** photostationary state mixture).

Light initiated *E-Z* and *Z-E* isomerization

Quantum yield determination

The *E-Z* isomerization quantum yield ($\Phi_{E\text{-}Z}$) of isatin diphenylhydrazone *E*-isomers ***E*1** and ***E*2** in DMF solution was determined by equations (6) and (7) at low *E*-Z conversion (to eliminate the effect of back *Z-E* photoisomerization): [58]

$$\phi_{E-Z} = \frac{\int_{c_0}^{c_t} dc}{\int_0^t I_a dt} = \frac{\Delta c}{\int_0^t I_a dt} \quad (6);$$

$$\Delta c = \frac{\Delta A_\lambda}{\varepsilon_{Z\,\lambda} - \varepsilon_{E\,\lambda}} \quad (7)$$

where: Δc is the concentration change in *E*- or *Z*-isomer, I_a is *E*-isomer absorbed photon flux at the irradiation wavelength λ using a monochromatic light source, ΔA_λ is the absorbance change at irradiation wavelength λ using a monochromatic light source, $\varepsilon_{E\lambda}$ is *E*-isomer molar extinction coefficient at irradiation wavelength λ using a monochromatic light source, $\varepsilon_{Z\lambda}$ is *Z*-isomer molar extinction coefficient at irradiation wavelength λ using a monochromatic light source and t is irradiation time. Because the *E*/*Z* conversion in the photostationary state is known from HPLC analysis (Table 2), the *Z*-isomer extinction coefficient at 405 nm was determined by Eq. (8):

$$\varepsilon_{Z\,405} = \frac{A_{405} - \varepsilon_{E\,405} c_E}{c_Z} \quad (8)$$

The *E*-isomer absorbed photon flux I_a during *E-Z* isomerization at irradiation wavelength λ = 405 nm and incident *E*-isomer concentration c_0 was calculated by Eq. (9): [59]

$$I_{a,E\,405} = I_0 \frac{\varepsilon_{E\,405}(c_0 - \Delta c)}{\varepsilon_{E\,405}(c_0 - \Delta c) + \varepsilon_{Z\,405}\Delta c}\left[1 - 10^{-\left[\varepsilon_{E\,405}(c_0 - \Delta c) + \varepsilon_{Z\,405}\Delta c\right]}\right] \quad (9)$$

The incident photon flux I_0 was determined by 2-nitrobenzaldehyde (2-NB) as chemical actinometer, according to Eq. (10): [60]

$$I_0 = \frac{k}{2.303\varepsilon_{o-NB\,405}\phi_{o-NB\,405} l}, \quad (10)$$

where: $\varepsilon_{o\text{-NB405}}$ is the molar extinction coefficient of 2-NB at irradiation wavelength 405 nm, $\Phi_{o\text{-NB405}}$ is the quantum yield of 2-NB photodegradation at irradiation wavelength, l is the path length and k is the 2-NB first-order photodegradation slope plotted under low-light-absorbing conditions: [60]

$$ln\left(\frac{[o-NB]_t}{[o-NB]_0}\right) = -kt \quad (11)$$

The *Z*-*E* isomerization quantum yield ($\Phi_{Z\text{-}E}$) of isatin diphenylhydrazone *Z*-isomers ***Z*1** and ***Z*2** in DMF solution was determined by Eq. (12):

$$\phi_{Z-E} = \phi_{E-Z}\frac{\varepsilon_{E\,\lambda}[E]}{\varepsilon_{Z\,\lambda}[Z]} \quad (12)$$

where: [*Z*] is the *Z*-isomer equilibrium concentration in the photostationary state, [*E*] is *E*-isomer equilibrium concentration in the photostationary state, $\varepsilon_{E\lambda}$ is *E*-isomer molar extinction coefficient at irradiation wavelength λ using a monochromatic light source, $\varepsilon_{Z\lambda}$ is *Z*-isomer molar extinction coefficient at irradiation wavelength λ using a monochromatic light source and $\Phi_{E\text{-}Z}$ is quantum yield of photochemical *E*-*Z* isomerization.

The incident photon flux I_0 at 465 nm was determined by ferrioxalate (FE) actinometry, according to Eq. (13): [61]

$$I_0 = \frac{I_{a,\,FE\,465}}{1-10^{-A_{FE\,465}}} = \frac{\left(\frac{dA_{FE\,390}}{dt}\right)\frac{1}{\phi_{FE\,465}\cdot\varepsilon_{FE\,390}\cdot\,l}}{1-10^{-A_{FE\,465}}} \quad (13)$$

where: $I_{a,\,FE465}$ is ferrioxalate actinometer absorbed photon flux, $A_{FE\lambda}$ is ferrioxalate absorbance at corresponding wavelength λ using a monochromatic light source, ε_{FE390} is ferrioxalate molar extinction coefficient at 390 nm, Φ_{FE465} is quantum yield of ferrioxalate photochemical conversion and l is the path length. Ferrioxalate absorbance at 465 nm ($A_{FE\,465}$) was measured by Ocean Optics SD2000 spectrophotometer.

SUPPORTING SCHEMES, TABLES AND FIGURES

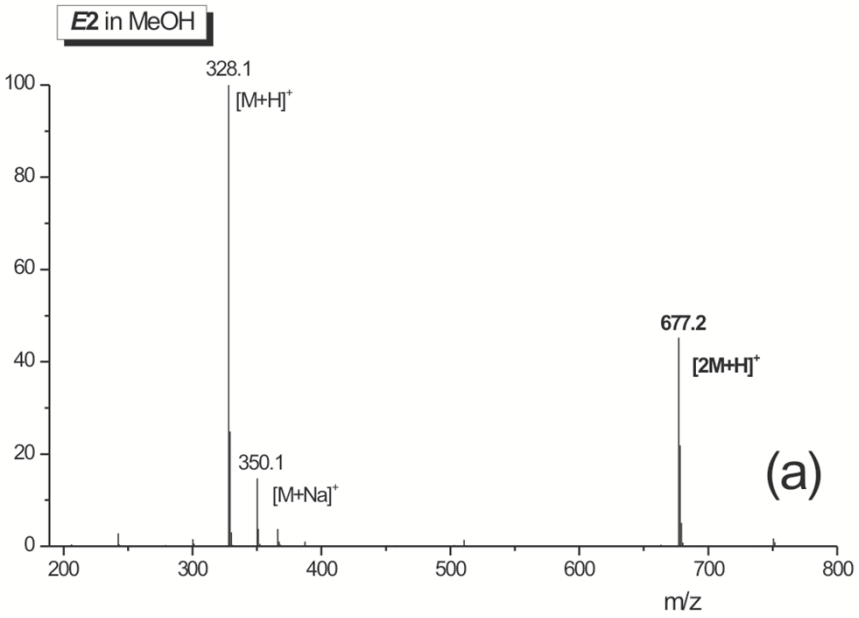

Fig. S1a. Mass spectrum of ***E*2** in MeOH (LC - MSD 6110, Agilent Technologies, MM (multimode ion source ESI/APCI), Positive ionisation mode, Full Scan).

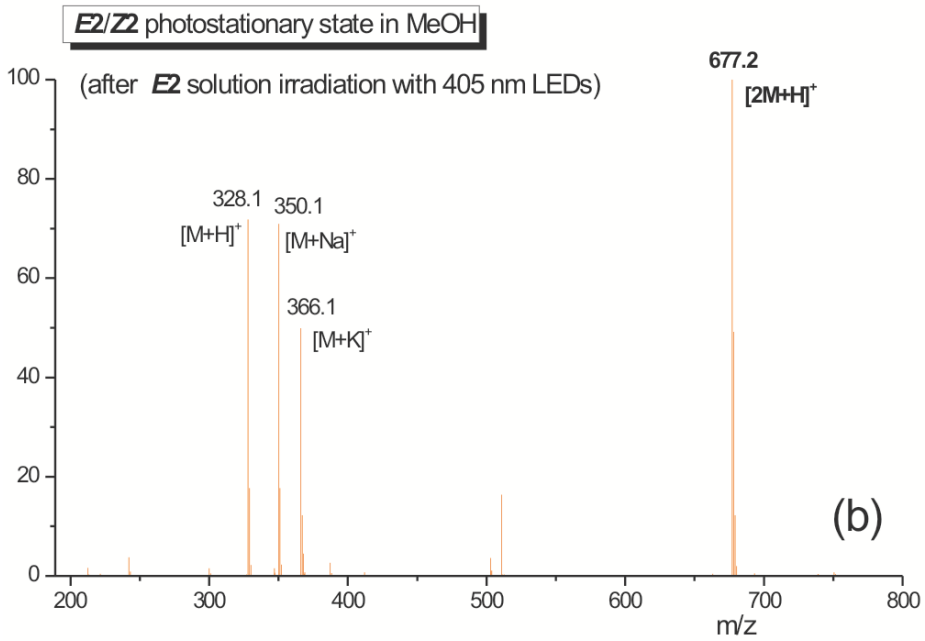

Fig. S1b. Mass spectrum of ***E*2** in MeOH after irradiation with light of 405 nm wavelength (LC - MSD 6110, Agilent Technologies, MM (multimode ion source ESI/APCI), Positive ionisation mode, Full Scan).

The presence m/z of $[2M+H]^+$ in Figs. S1a, S1b in ***E*2** methanolic solution clearly indicates the existence of the ***E*2** dimer, contrary to polar aprotic MeCN (Fig. S1c).

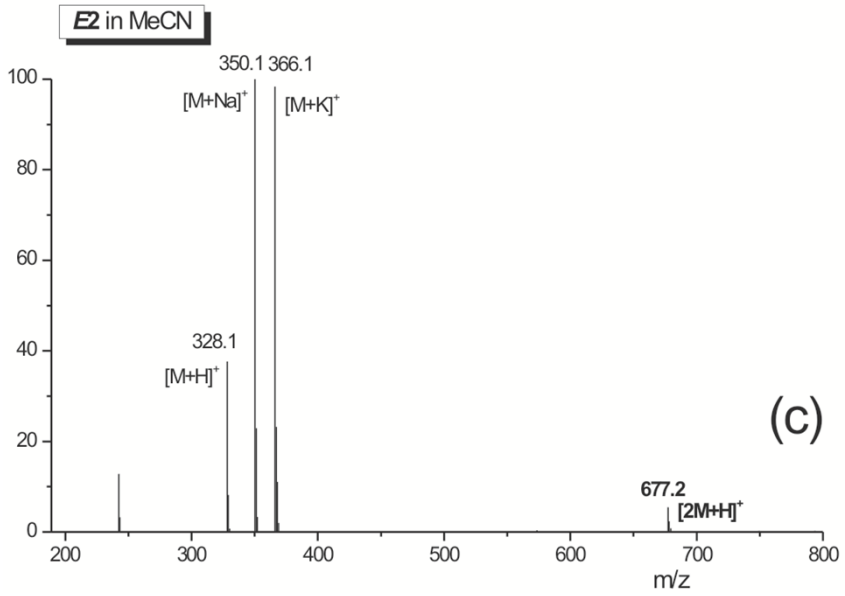

Fig. S1c. Mass spectrum of ***E*2** in MeCN (LC - MSD 6110, Agilent Technologies, MM (multimode ion source ESI/APCI), Positive ionisation mode, Full Scan).

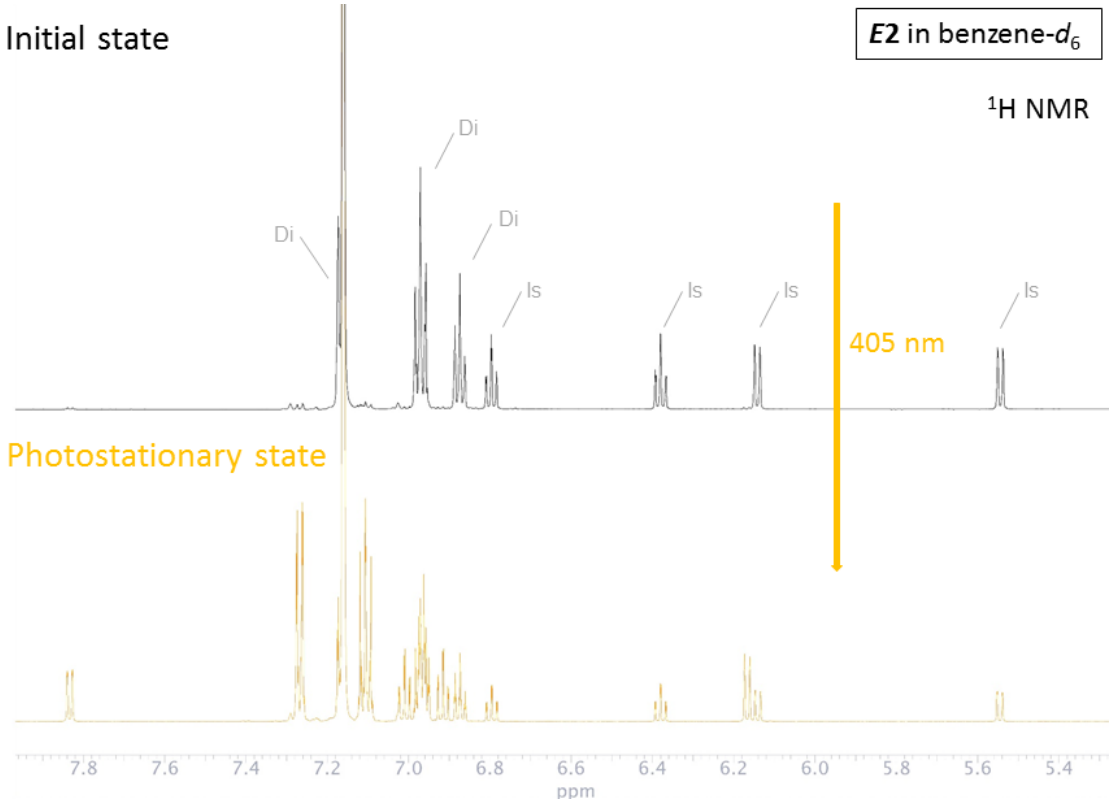

Fig. S2. ^{1}H NMR spectrum of ***E*2** in benzene-d_6 before and after irradiation with light of 405 nm wavelength (Di –diphenylamino protons; Is –isatin protons; T = 298.15 K).

The multiplet splitting of diphenylamino protons in the photostationary state speaks about their unequeality in ***Z*2** isomer. During the photoisomerization cycles, the reversible changes in integration intensities for non-overlapping protons were observed.

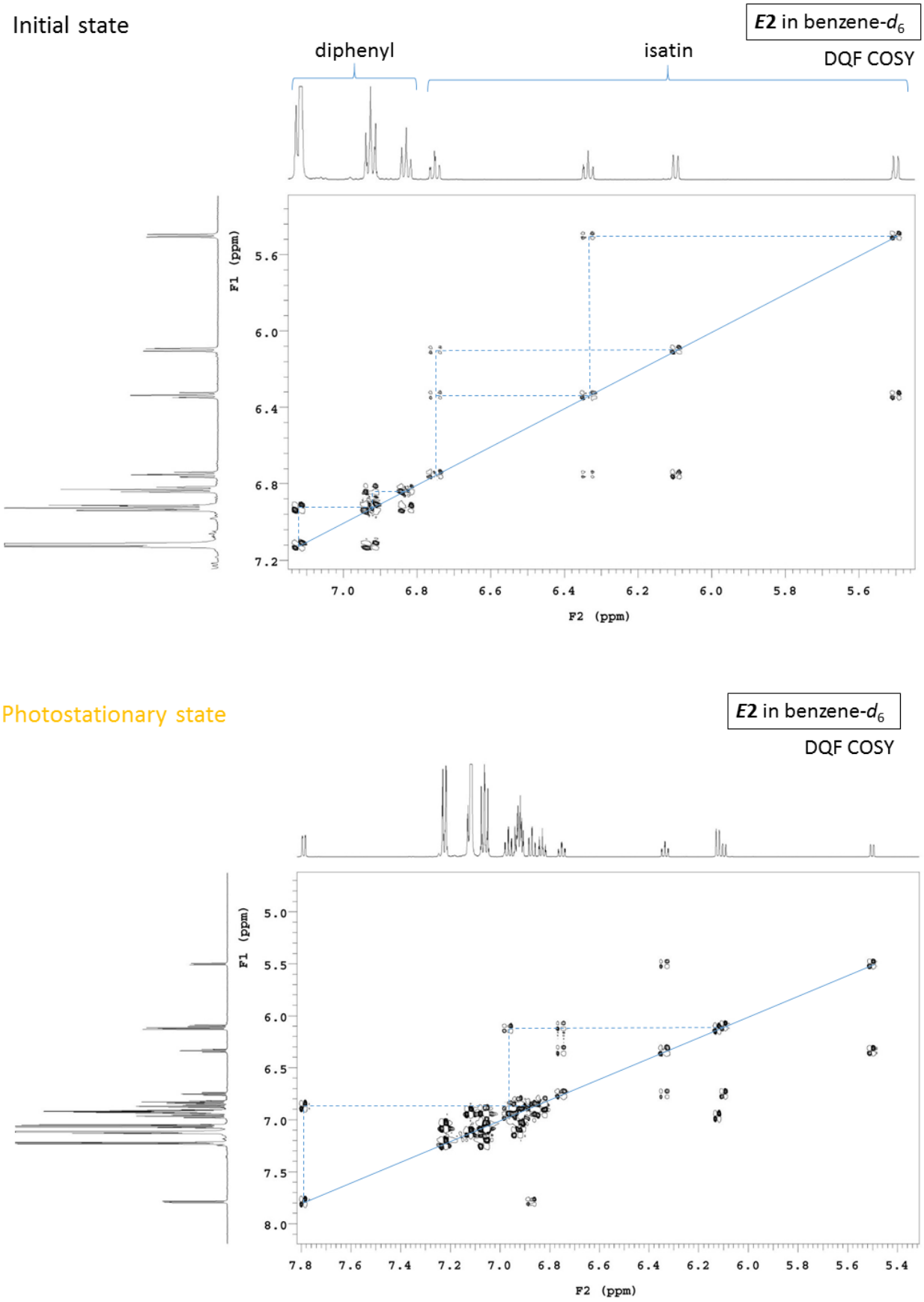

Fig. S3. 2D ^{1}H-^{1}H COSY spectrum of ***E*2** in benzene-d_6 before and after irradiation with light of 405 nm wavelength (T = 298.15 K).

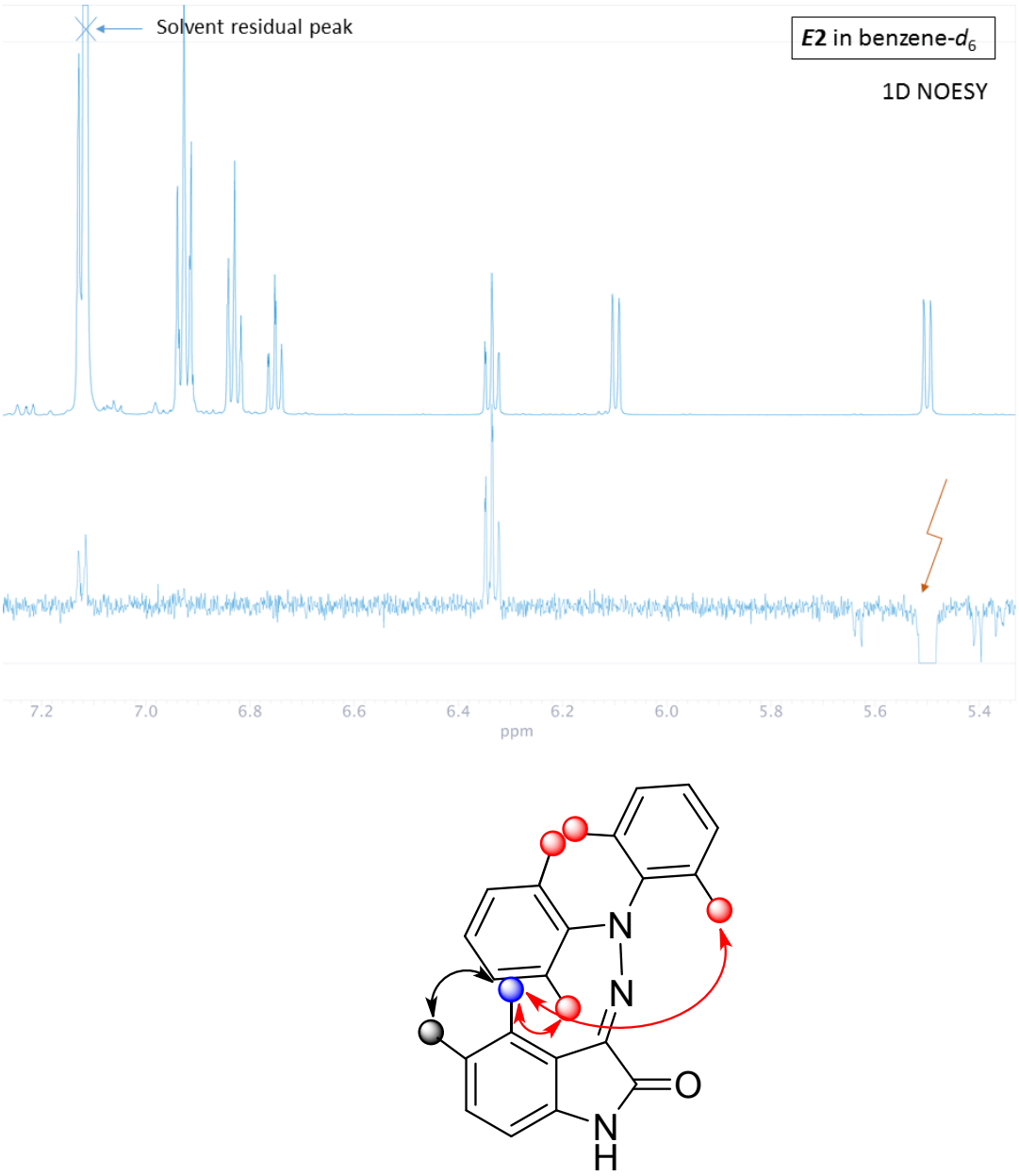

Fig. S4. ^{1}D NOESY spectrum of ***E*2** in benzene-d_6 (T = 298.15 K) and schematic structure describing NOE interactions.

Irradiated proton at 5.5 ppm (blue circle) shows two interactions with protons at approximately 6.3 ppm (isatin proton – black circle) and ~7.1 (phenyl ring protons in *orto*-position – red circles). The NOE interaction with phenyl protons indicates the shielding from phenyl rings. Therefore we assume that the biphenyl rings are in „scissor-like" structure above the isatin skeleton and are equivalent.

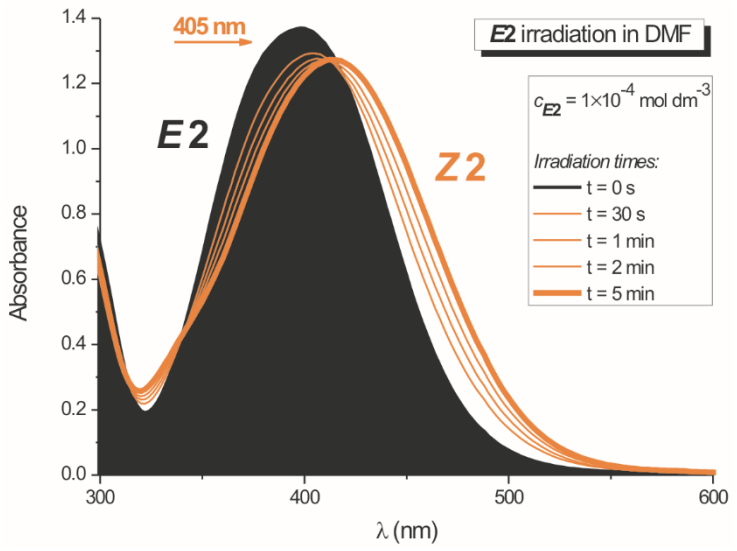

Fig. S5. The UV-Vis spectrum of N^1-methylisatin N^2-diphenylhydrazone *E*-isomer ***E2*** in DMF before and during the irradiation with visible light of 405 nm wavelength ($\boldsymbol{c_{E2}}$ = 1×10^{-4} M; 1 cm cuvette; T = 298.15 K).

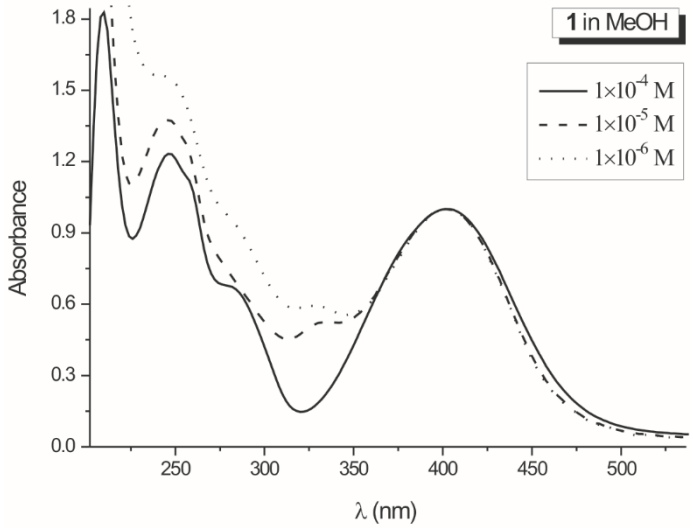

Fig. S6a. Normalized spectra of ***E*1** in MeOH at various hydrazone ***E*1** concentrations (10^{-4}, 10^{-5} and 10^{-6} M; 1 cm cuvette; T = 298.15 K).

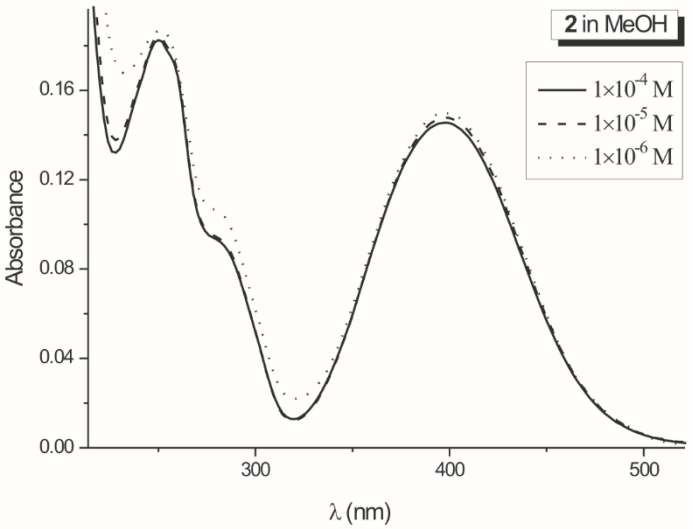

Fig. S6b. Normalized spectra of ***E*2** in MeOH at various hydrazone ***E*2** concentrations (10^{-4}, 10^{-5} and 10^{-6} M; 1 cm cuvette; T = 298.15 K).

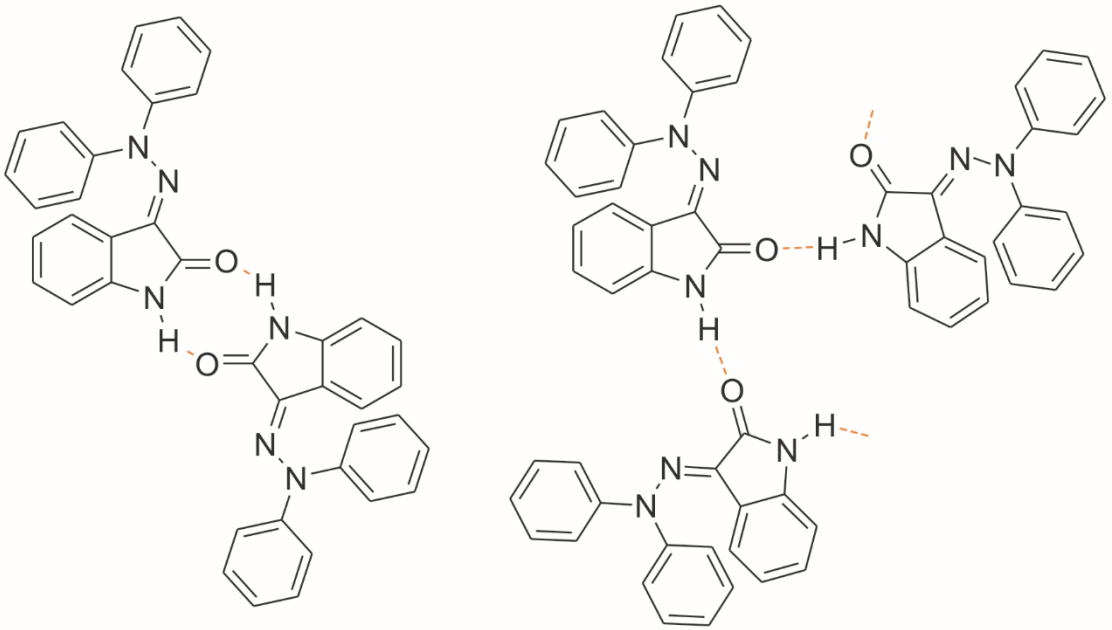

Scheme S1. Assumed structure of dimers or higher aggregates (*n*-mers) of ***E*1** at higher concentrations.

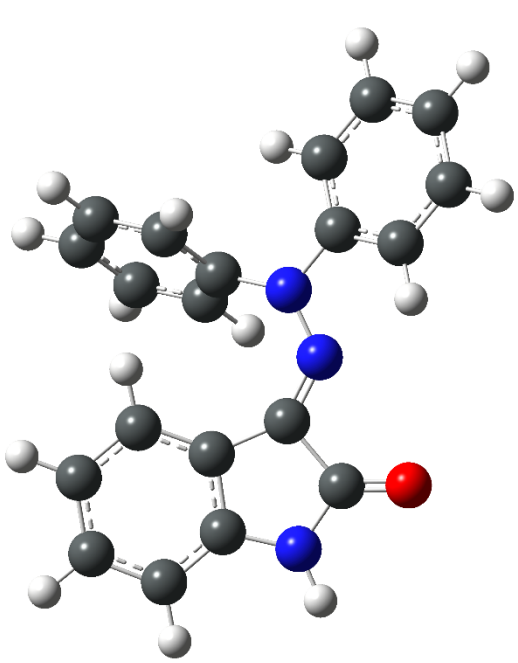

***E*1**

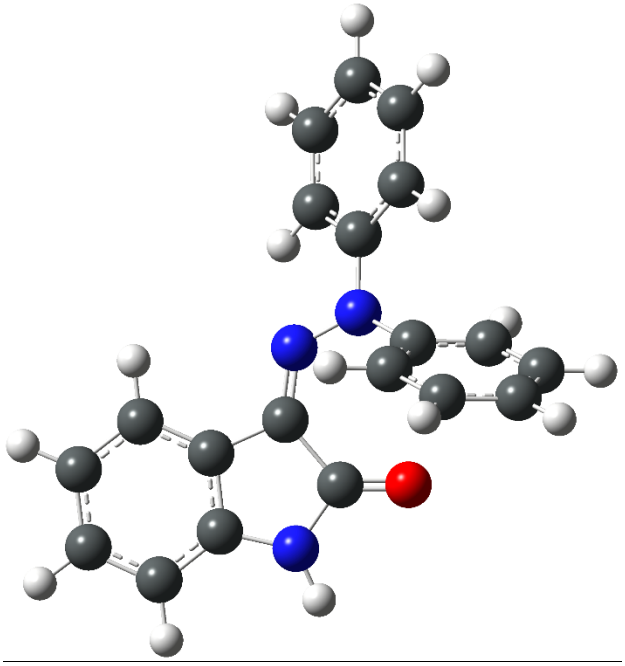

***Z*1**

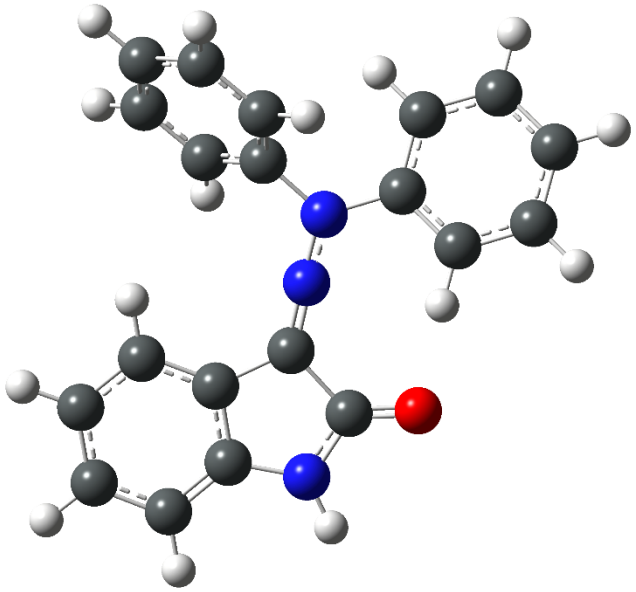

***E*1*Z*1TS**

Scheme S2. Calculated geometries of ***E*1** and ***Z*1** isomers and corresponding transition state for their mutual *E*-*Z* and *Z*-*E* thermal isomerization in DMF at the M062x 6-31+g(dp)//M062X/6-311++G(d,p) level (T = 298.15 K; TS – transition state).

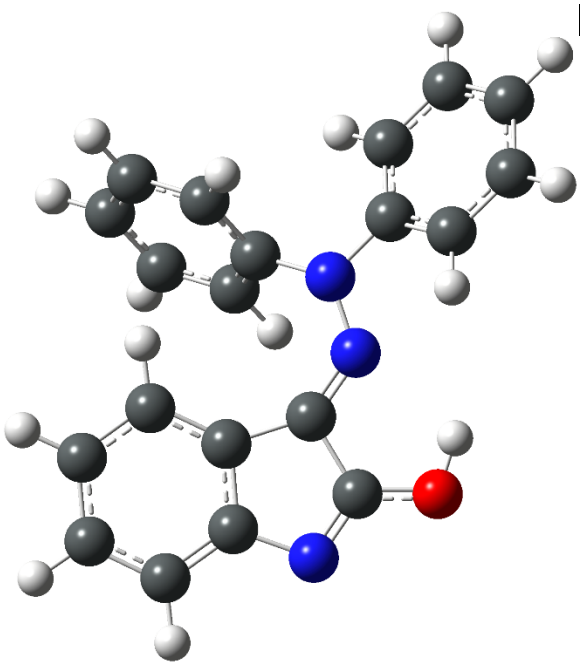

***E*1-enol**

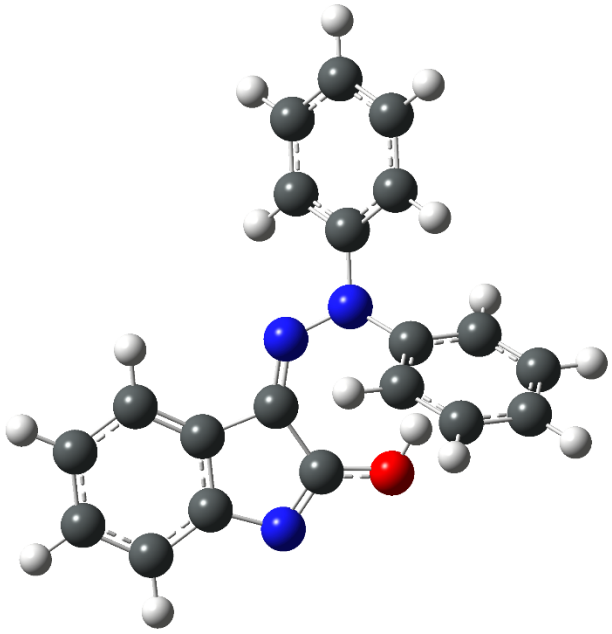

***Z*1-enol**

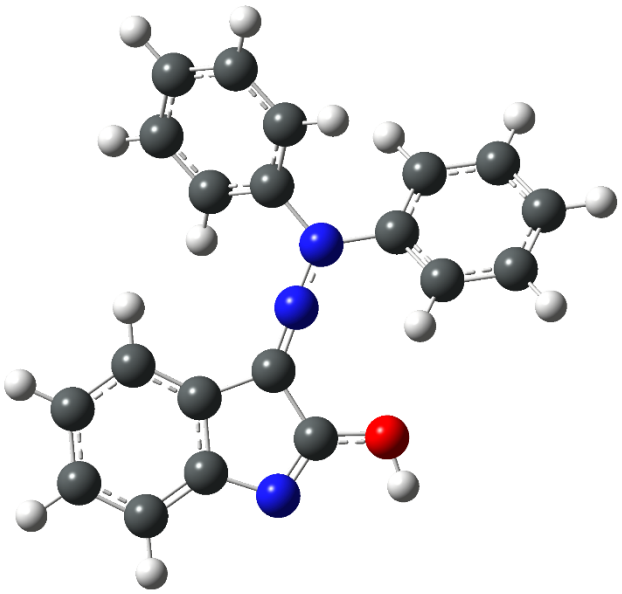

***E*1-enol*Z*1-enolTS**

Scheme S2. Calculated geometries of ***E*1** and ***Z*1** enol conformers ***E*1-enol** and ***Z*1-enol** and corresponding transition state for their mutual *E-Z* and *Z-E* thermal isomerization in DMF at the M062x 6-31+g(dp)//M062X/6-311++G(d,p) level (T = 298.15 K; TS – transition state).

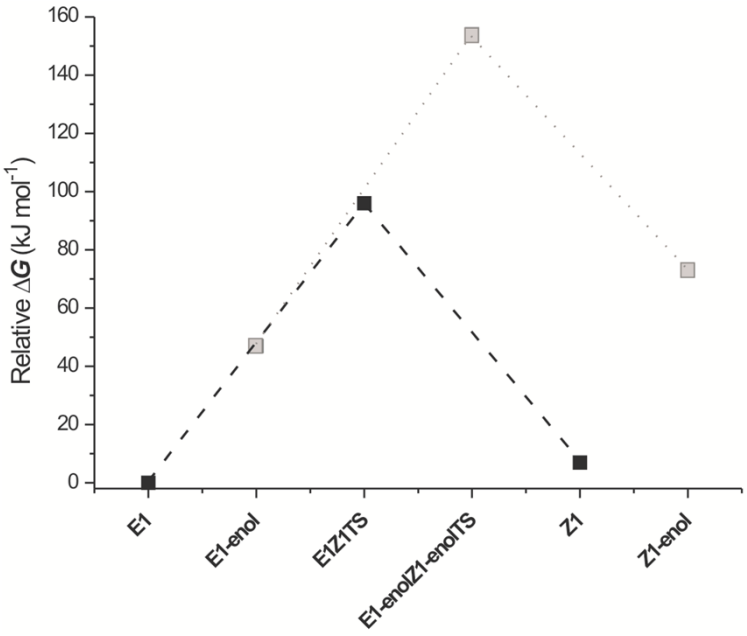

Fig. S7. Calculated relative Gibbs free energies of ***E*1** and ***Z*1** isomers and their enol conformers ***E*1-enol** and ***Z*1-enol** at the M062x 6-31+g(dp)//M062X/6-311++G(d,p) level (T = 298.15 K; TS – transition state).

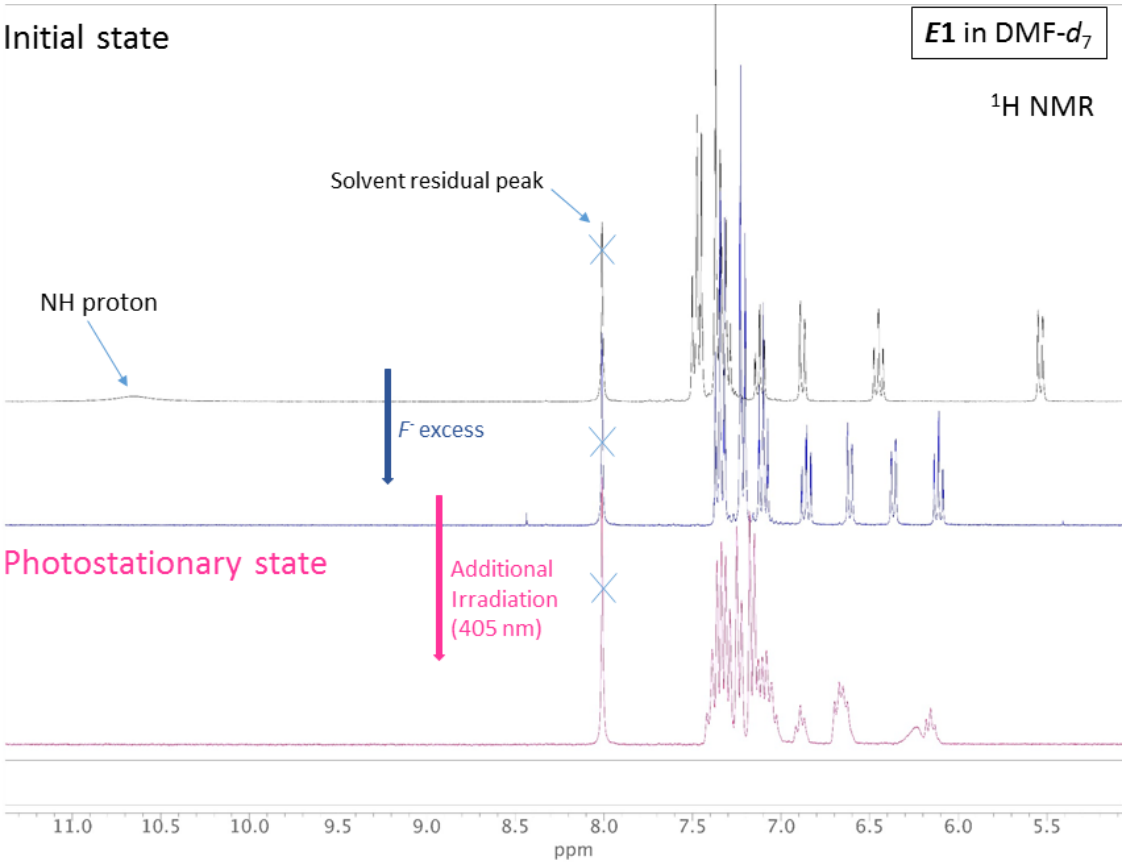

Fig. S8. ^{1}H NMR spectrum of ***E*1** in DMF-d_7 before and after F^- anion addition, followed by irradiation with light of 405 nm wavelength (T = 298.15 K).

Enolate formation

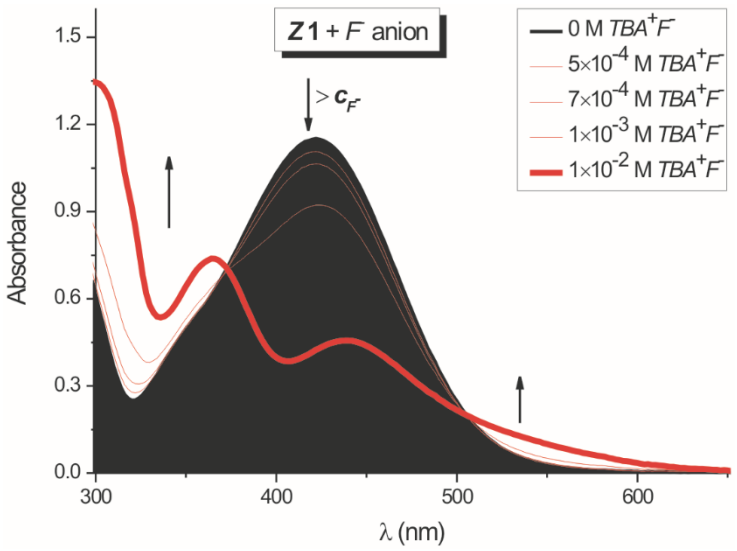

Fig. S9. Concentration influence of F^- anion on the UV-Vis spectrum of isatin N^2-diphenylhydrazone ***E*1**/***Z*1** photostationary state 40:60 mixture (solvent: DMF; $c_{E1\text{-initial}}$ = 1×10^{-4} M; 1 cm cuvette; T = 298.15 K).

The enolate (not enol) formation after F^- (or OH^-) addition is supported by the following statements:

1. The presence of enolic OH signal is not observed in ^{1}H NMR spectrum in DMF-d_7 nor in CD_3CN (due to the intermolecular hydrogen bonding with F^- anion after anion addition, the signal (singlet) with chemical shift above 4 ppm should appear). The overall number of signals for ***E*1** decreased from 15 to 14 (4 signals from isatin (not 5) and 10 for diphenyl) after the F^- anion addition.

2. Without the strongly basic anion addition, the presence of enol form (equilibrium between enol and keto tautomer) was not observed even in highly polar solvents. Moreover, the weakly basic anion excess (that significantly increases the ionic strength and thus dielectric constant) does not affect the UV-Vis spectra of *E*-isomer ***E*1** solution (contrary to strongly basic anions).

Table S1. Relative Gibbs free energies of compounds **3** and **4** formed from ***E*1** and ***Z*1** isomers (at high F^- anion excess), respectively, calculated at the [M062x 6-31+g(dp)/M062X 6-311++G(dp)] level in vacuum (T = 298.15 K).

	ΔG kJ mol^{-1}
3	4
4	0

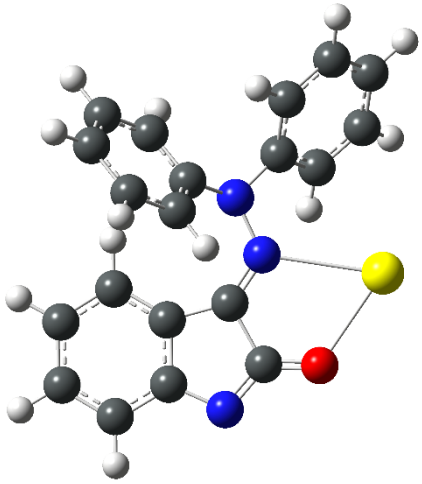

3

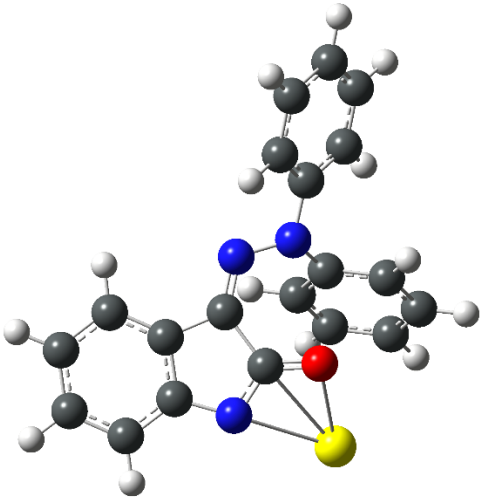

4

Structure of compound 4

Structure of compound **4** formed from *Z*-isomer ***Z*1** at high F^- anion excess could be also represented by the following form **b** that includes anion-π-cation interaction (Scheme S3). The experimental evidence for such interaction type was already published by Dennis A. Dougherty. [33] However, the existence of ***Z*1** form **b** was excluded based on its markedly higher energy compared to form **a** (calculated ΔE = 138 kJ mol^{-1}):

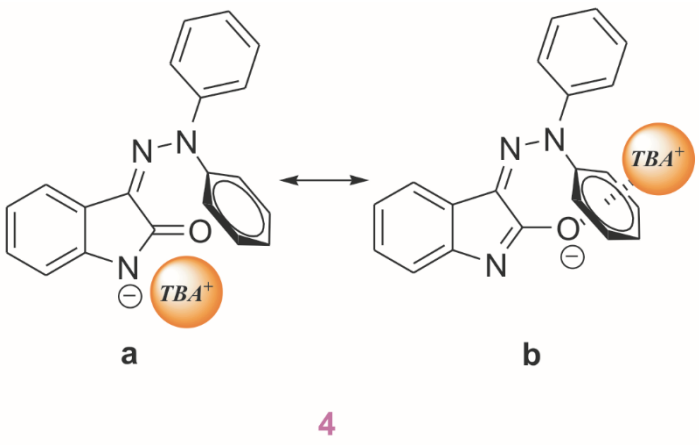

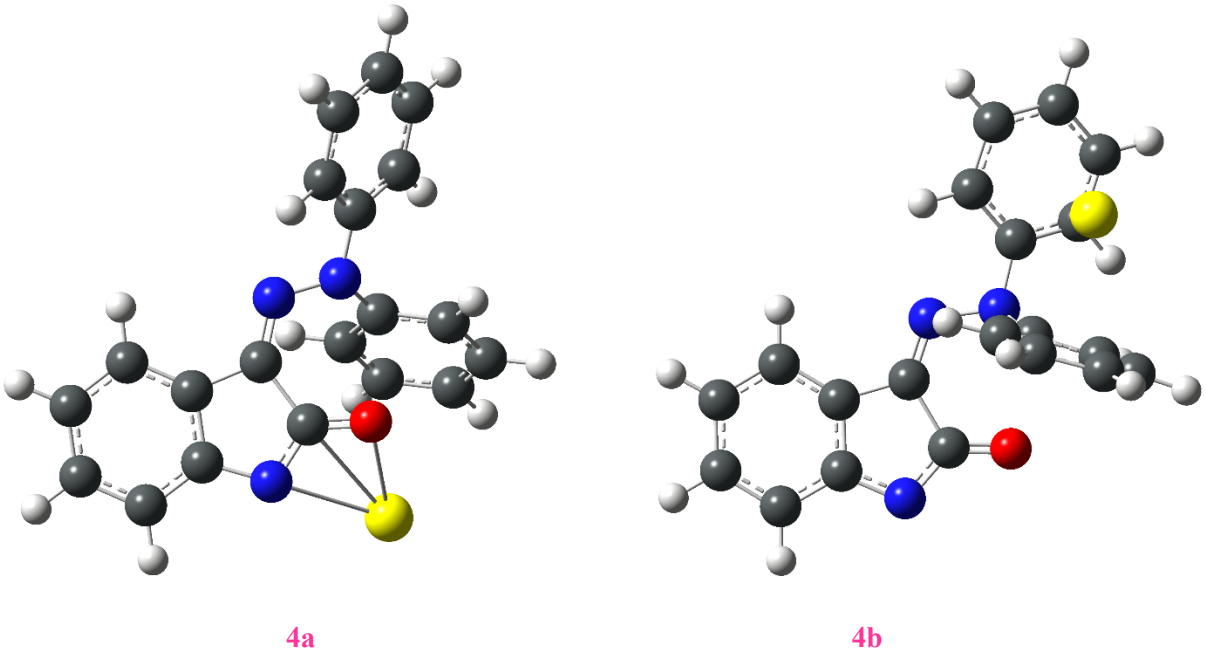

Scheme S3. Possible structures of compound **4** formed from *Z*-isomer ***Z*1** at high F^- anion excess (for simplification of energy calculation, the TBA^+ cation was replaced by K^+ cation; element colour in optimized geometries: carbon – grey, hydrogen – white, oxygen – red, nitrogen –blue and potassium cation – yellow).

From the practical point of view, the TBA^+ replacement with other cation is interesting. We assume that the negative charge delocalization in –N-C=O structural fragment of **4a** depends mostly on the cation size and its polarizability. However, this assumption was not confirmed experimentally due to the low solubility of *KF*, *LiF* and $ZnCl_2$ salts in DMF or MeCN (free F^- anion concentration does not exceed the critical value of 10^{-2} M).

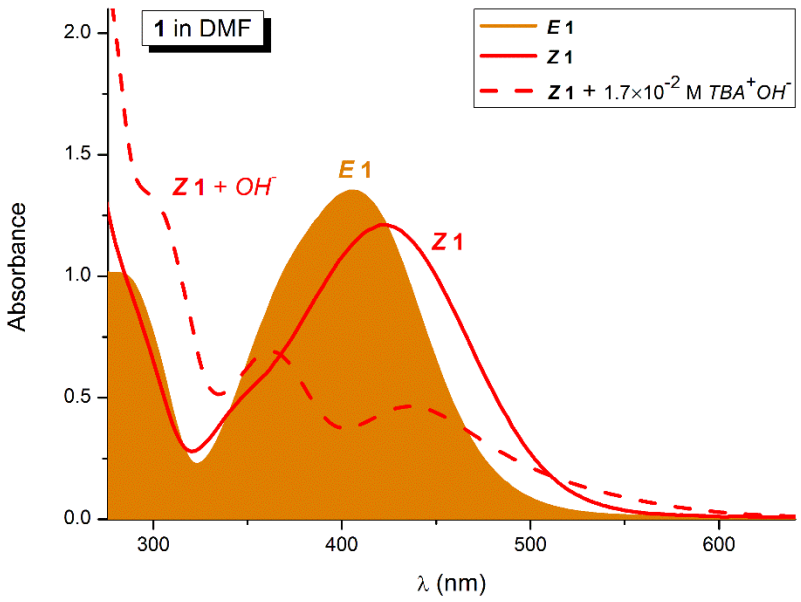

Fig. S10. Concentration influence of OH^- anion on the UV-Vis spectrum of isatin N^2-diphenylhydrazone ***E*1**/***Z*1** photostationary state 40:60 mixture in DMF ($c_{E1\text{-initial}}$ = 1×10^{-4} M; 1 cm cuvette; T = 298.15 K).

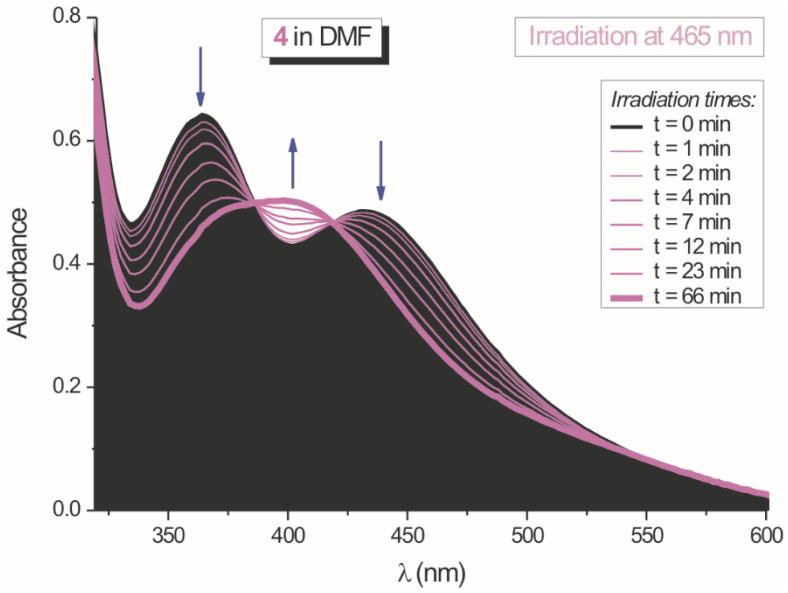

Fig. S11. Dependence of the UV-Vis spectra of hydrazone **4** on the irradiation time in DMF (λ_{exc} = 465 nm; $c_{E1\text{-initial}}$ = 1×10^{-4} M; c_{F^-} = 1×10^{-2} M; 1 cm cuvette; T = 298.15 K).

ADDITIONAL REFERENCES

[57] W.H. Press, S. Teukolsky, W. Vetterling, B. Flannery, Numerical Recipes: The Art of Scientific Computing, Cambridge University Press, New York, 2007.

[58] Wolfram Research, Inc., Mathematica, Version 9.0, Champaign, IL, 2012.

[59] P. Klán, J. Wirz, Spectrophotometric Determination of the Reaction Progress, in: J. Coxon, P. Bailey, L. Field, J.A. Gladysz, P. Parsons, P. Stang (Eds.), Photochemistry of Organic Compounds: From Concepts To Practice, John Wiley & Sons Ltd, 2009, Chichester, pp. 114-116.

[60] E.S. Galbavy, K. Ram, C. Anastasio, 2-Nitrobenzaldehyde as a chemical actinometer for solution and ice photochemistry, *J. Photochem. Photobiol. A Chem.*, 2010, **209**, 186-192, http://dx.doi.org/10.1016/j.jphotochem.2009.11.013.

[61] T. Lehóczki, É. Józsa, K. Ösz, Ferrioxalate actinometry with online spectrophotometric detection, *J. Photochem. Photobiol. A Chem.*, 2013, **251**, 63-68, http://dx.doi.org/10.1016/j.jphotochem.2012.10.005.